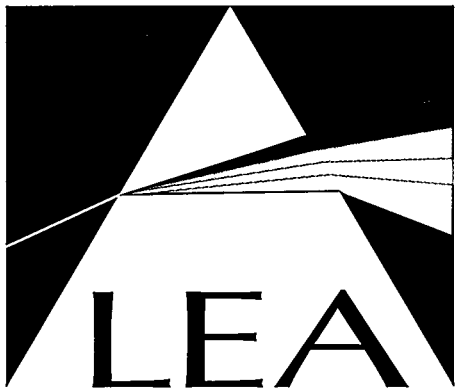

Laboratory for Experimental Astrophysics

UCRL-JC-119291

Low-Energy Response of Superconducting Tunnel Junction X-ray Spectrometers

Simon E. Labov, L.H. Hiller, C.A. Mears, M. Frank, H. Netel and F. Azgui
Laboratory for Experimental Astrophysics
Lawrence Livermore National Laboratory
P.O. Box 808, L-401, Livermore, CA 94550, USA

A.T. Barfknecht
Conductus, Inc.
969 West Maude Ave., Sunnyvale, CA 94086, USA

Prepared for the
Applied Superconductivity Conference
October 16–21, 1994
Boston, MA

December 9, 1994

Applied Superconductivity Conference, Boston, MA, 16-21 October 1994, to be published in IEEE Trans. Appl. Supercond.

Low-Energy Response of Superconducting Tunnel Junction X-ray Spectrometers

Simon E. Labov, L. H. Hiller, C. A. Mears, M. Frank, H. Netel and F. Azgui
Laboratory for Experimental Astrophysics, Lawrence Livermore National Laboratory, Livermore, CA USA

A. T. Barfknecht
Conductus, Inc., Sunnyvale, CA, USA

Abstract—**Thin film structures incorporating metallic superconducting layers and tunnel junctions can be configured as low-energy X-ray spectrometers. We present results obtained when low-energy X-rays are absorbed in niobium films coupled to aluminum layers that serve as quasiparticle traps in an Nb/Al/Al_2O_3/Al/Nb tunnel junction X-ray detector. The linearity of the pulse height as a function of energy is discussed along with the energy dependence of the observed resolution and its relation to the broadening mechanisms. A resolution of 14 eV at 1 keV has been measured with our detector cooled to 0.3 K.**

I. Introduction

Superconducting X-ray spectrometers are being developed to exploit the small binding energy of Cooper pairs in order to measure the energy of X-ray photons with great precision. In a superconducting-insulator-superconducting tunnel junction X-ray spectrometer, single X-ray photons are absorbed in a superconductor resulting in a nonequilibrium distribution of quasiparticles and phonons. The number of quasiparticles produced is proportional to the X-ray energy. When the superconductor is cooled far below the critical temperature, and the Cooper pair tunneling is suppressed by a magnetic field, the current flowing through the insulating barrier is proportional to the density of these nonthermal quasiparticles.

We describe here results obtained with a superconducting detector designed to investigate the various noise sources that contribute to the detector's X-ray resolution. The device is small, about 0.1 mm by 0.1 mm, to minimize the capacitance and therefore the electronic amplifier noise. To ensure high quality of the superconductors, the device is fabricated with films less than 300 nm thick. The resulting device is only a moderately efficient X-ray detector, but all the concepts and technology used here can be combined with larger, more efficient superconducting absorbers [1, 2]. We find that irradiating the detector with X-rays with a large range in energy can be a valuable diagnostic technique for studying superconducting tunnel junction X-ray detectors.

II. Detector Design and Fabrication

The detector was fabricated at Conductus, Inc. using a modification of our standard photolithographic niobium-aluminum trilayer process [3]. A silicon wafer was thermally oxidized and a 250 nm layer of niobium was sputter-deposited, followed by 200 nm of aluminum. The aluminum was oxidized, and then another 200 nm of aluminum were deposited, followed by 160 nm of niobium. After etching the detector pattern and the bottom wiring layer, a 600 nm layer of SiO_2 dielectric was deposited, and small 5 μm contact holes to the top Nb layer were masked and etched. A 1 μm thick wiring layer of Nb was deposited, patterned and etched. The wiring traces leaving each junction are only 5 μm across to prevent quasiparticles from leaving the detector through the leads. The detector cross section is shown in Fig. 1., and the detector fabrication is described in more detail in [4].

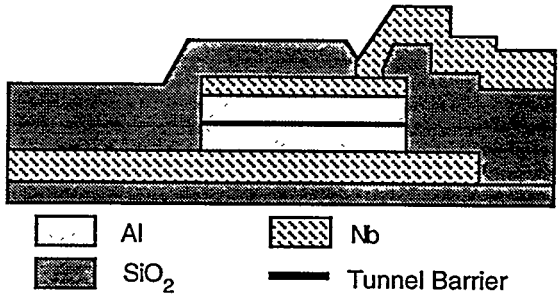

Fig 1. Cross-section of the detector. The top niobium layer is 160 nm thick, and the bottom layer is 250 nm thick. The thickness of the two aluminum trapping layers is 200 nm.

The junction was patterned in a sinusoidal shape. Sinusoidal and higher order polynomial patterns can be used to reduce the magnetic field required to suppress the dc Josephson current [5, 6]. In practice, the curved shape results in a more complex pattern of Fiske mode structures, and the same magnetic field is required as would be used with a simple straight-edged diamond-shaped structure.

When an X-rays is absorbed in the top or bottom niobium layers, a cloud of quasiparticles is created which diffuses into the aluminum layer where the quasiparticles relax and become trapped. This quasiparticle trapping concentrates the quasiparticles near the barrier, and increases the tunneling rate and therefore the magnitude of the X-ray induced current pulse. By placing aluminum trapping layers on both sides of the barrier, we increase the duration of the current pulse [7]. When an X-ray is absorbed in one of the aluminum films, the photoelectron will typically reach one of the niobium films before stopping, thereby spreading the initial cloud of quasiparticles into both the niobium and the aluminum.

Manuscript received October 18,1994.
This work was performed under the auspices of the U. S. Department of Energy by Lawrence Livermore National Laboratory under contract No. W-7405-ENG-48 with additional support from NASA contract NAS5-38013 and NASA grant number NAGW-3907

III. Detector operation

When measured at 4.2 K, the current-voltage characteristics of the device exhibits supercurrent at zero voltage and kinks at the sum-gap voltage. The appearance of these features above the critical temperature of bulk aluminum indicate that the proximity effect has elevated the energy gap, Δ, and the transition temperature, T_c, of the aluminum films. As the temperature was lowered, the gap voltage increased to its low-temperature value of $\Delta = 0.34$ meV, about twice the value of Δ in bulk aluminum.

As the junction is cooled, the density of thermally excited quasiparticles drops, thereby reducing the current at voltages $V < 2\Delta$. Below a temperature of about 0.24 K, this sub-gap current becomes insensitive to changes in temperature. At such temperatures, the measured current is due to micro-shorts and/or small normal regions where the magnetic field has penetrated the device. We characterize the integrity of the insulating barrier with a quality factor $Q = R_d/R_n$, where R_d is the low temperature limit of the dynamic resistance, and R_n is the normal resistance of the junction. The device described here has $R_n = 0.14\ \Omega$, and below 0.24 K the sub-gap current was 0.3 nA at 0.25 mV with $R_d = 830\ k\Omega$, and $Q = 6 \times 10^6$.

A. Detector and Electronics Configuration

The detector was cooled in an adiabatic demagnetization refrigerator which includes shielding to minimize both the refrigerator's and the Earth's magnetic field at the detector. After reaching the desired operating temperature, a magnetic field of 2.5 mT was applied in the plane of the junction to suppress the dc Josephson current. The temperature was stabilized at 0.3 K, and the detector biased at 0.3 mV with 24 nA of current. While the sub-gap current was slightly lower at temperatures below 0.3 K, the resolution was not significantly different.

A current-sensitive preamplifier was used to measure the X-ray induced current pulses. The amplifier was configured with a 0.45 μs response time, and filtered by an 8 pole Bessel filter limiting the electronic bandwidth to between 1 kHz and 250 kHz. The upper limit to the electronic bandwidth was set to minimize high frequency noise, while not significantly integrating the current pulses. We found that additional integration did not improve the overall signal to noise ratio. This may be due in part to the statistical fluctuations associated with multiple tunneling and the quasiparticle loss mechanism [8, 9]. The X-ray-induced current pulses were typically 0.6 μA high for 6 keV X rays, with a 5 μs decay time. Once filtered, the pulses were fed directly into a pulse-height analyzer and a spectrum was produced in real time.

B. X-ray Source

X rays were produced by a low-power electron beam impacting a target anode at high voltage. The emission current was typically 0.1 mA, and the electrons were accelerated by 1.5 to 10 kV. We used targets of aluminum, copper and titanium, and coated these with a variety of compounds including NaCl, KCl, $CaSO_4$, MgO, Si, SiO_2, and C. The source produces both line emission characteristic of the target material, and bremsstrahlung continuum radiation. The shape of the bremsstrahlung radiation, and the intensity of the various emission lines, depend strongly on the target voltage.

The X rays passed through a high vacuum line into the cryostat. The X rays were not collimated and hit all parts of the detector with equal intensity. Three thin filters were deployed to block infrared radiation from the room-temperature vacuum line and the hot target anode. Each filter consisted of a polyester film, 1.2 μm thick, with a 12 nm aluminum coating. One filter was mounted on the 77 K shield of the cryostat, and one was mounted on the 2 K shield just inside of the 77 K shield. A third filter was mounted on the magnetic shield that excludes the Earth's field from the detector. The three filters together transmit 72% of the X rays at 2 keV, dropping to 11% at 1 keV, and dropping to mostly below 1% at lower energies with the notable exception at the carbon K edge (E = 284 eV) where the combined filter transmission jumps up to 6.6%, and then drops again at energies below 280 eV.

The detector used here is coated with 600 nm of SiO_2. This layer also limits the low energy efficiency of this particular test device, transmitting 80% at 2 keV, 65% at 1 keV, and 7.3% at 280 eV. To extend the operating range of the superconducting tunnel junction X-ray detector, we can thin, or possibly eliminate the SiO_2 layer over the photon absorbing layer, and use thinner filers.

IV. X-ray results

We have measured the from a number of different electron-beam target anodes. Most X-ray lines produced two peaks, one from X rays absorbed in the top Nb layer, and a separate peak from X rays absorbed in the lower Nb layer. The notable exception was the C Kα line at 282 eV. At this energy, the X-rays can not penetrate through the upper Nb layer, and only one peak is observed.

There is a subtle difference between the shapes of the pulses produced by X rays absorbed in the top film, and X rays absorbed in the bottom layer. As discussed elsewhere [10, 11] this difference in the pulse shape can be used to discriminate between events occurring in the two layers. Furthermore, as we move from test devices to prototype detectors, we will be using thicker and larger superconducting absorbers that are not necessarily directly on top of the tunnel junction structure. All the X rays at a given energy absorbed in such a device will produce a single peak [2]. With our current test detectors, the two sets of peaks turn out to be quite useful. They allow us to study the behavior of each film independently, and as shown below, there are some striking differences.

To accurately determine its position, height and width, each peak was fit with a Lorentzian profile. Fitting the peaks also allowed the error in these measurements to be estimated. In most cases, a Lorentzian profile provided a good fit. In all cases, the fit values were very close to estimates made by other techniques. Some of the peaks at higher energies were too weak to accurately measure the width, so only the

position of these peaks are used in the analysis presented here.

The spectra described here were accumulated from different electron-beam target anodes, and from a ^{55}Fe source. The peak positions for X rays absorbed in the top Nb layer, and the bottom Nb layer are shown as a function of energy in Fig. 2a. Also shown in Fig. 2a are the straight-line weighted fits for each layer. The deviations from linearity can be seen in Fig. 2b where the residuals to the fits in Fig 2a are plotted.

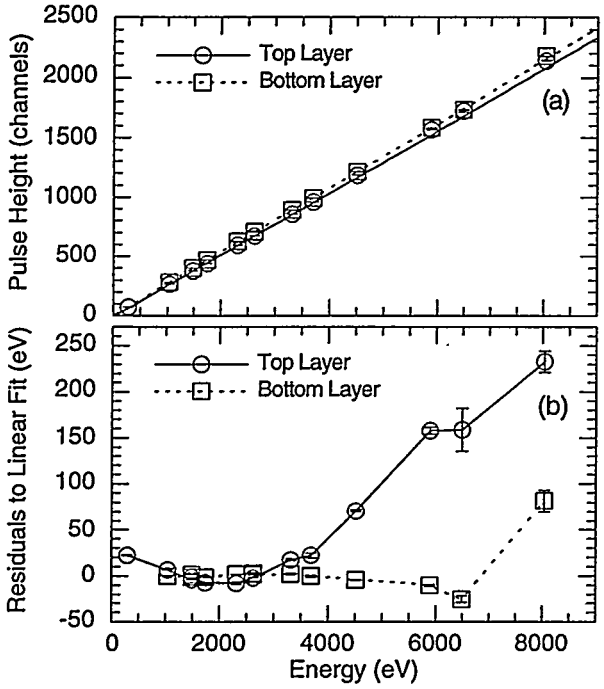

Fig 2. The linearity of the detector is shown in (a) for X-rays absorbed in the top and the bottom niobium layers. The residuals in (b) were calculated by subtracting the X-ray energy from the energy values determined by a weighted linear fit. For clarity, lines are drawn between the points in (b).

The detector is very stable. Several energies were measured more than once at different times during the day. No significant gain change was observed. In fact, the next day the detector was warmed above its critical temperature, and then re-cooled to 0.3 K. The same magnetic field and bias were applied, and the spectra produced were nearly identical. The gain shift between the two days was less than 0.7 %.

Two examples of X-ray spectra are shown in Figs. 3 and 4. In addition to the characteristic X-ray lines, each spectrum includes a peak obtained by injecting current with an electronic pulser during the X-ray measurements. This allows us to monitor the noise contribution from our electronics. With this test detector, X rays with energy larger than about 1 keV will often be absorbed in the substrate underneath and nearby the junction. These X rays excite phonons in the substrate, and some of those phonons are absorbed in the superconducting layers producing quasiparticles. This will contribute, along with any bremsstrahlung radiation, to a large number of pulses observed with small pulse heights.

In Fig. 3 we show the spectra obtained with an Al target coated with NaCl and C, and at a potential of 5 kV. In Fig. 4 we show the spectrum from the same anode, but with the voltage set to 1.5 kV to reduce the emission of Al and Cl Kα X rays, and hence the number of small pulses they produce when absorbed in the substrate, as well as low-energy bremsstrahlung radiation. With the X-ray source at 1.5 kV, the number of counts with low pulse heights is thus reduced, and it is possible to see the C Kα emission line at E = 282 eV. Since C Kα X rays are only absorbed in the top film, we see only one C Kα emission peak.

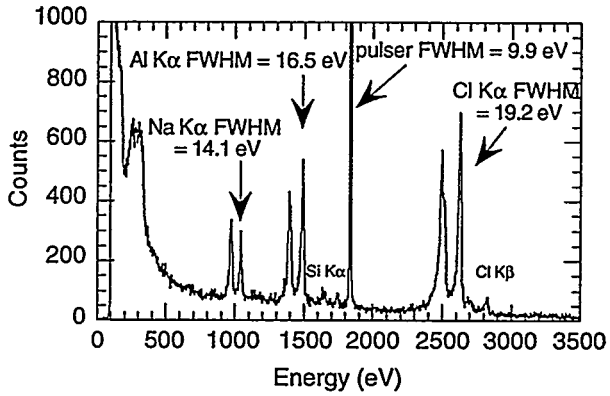

Fig. 3. The spectrum using an Al anode coated with C and NaCl. The anode voltage was 5 kV, and the detector temperature was 0.3K. The pairs of peaks are due to the different response from X rays absorbed in the top Nb layer (lower energy peak), and X rays absorbed in the bottom Nb layer (higher energy peak). The energy scale has been set by the peaks from absorption in the bottom layer.

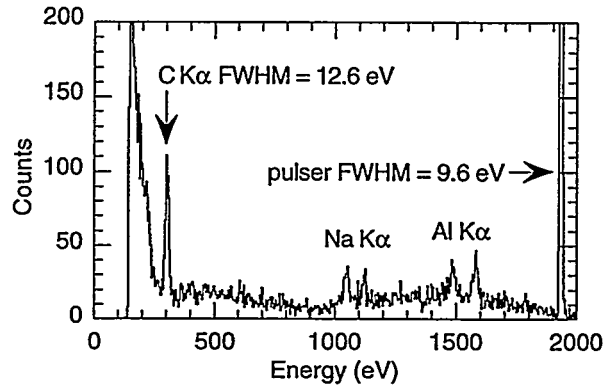

Fig. 4. The spectrum from an Al anode coated with C and NaCl. The anode voltage was 1.5 kV, and the detector temperature was 0.3K. The energy scale has been set by the peaks from absorption in the top layer.

The resolution measured for the lines shown above, and several more are summarized in Fig. 5. The resolution was 14.1 eV FWHM at 1 keV, and ranged from 12.6 eV FWHM at 0.28 keV to 22 eV at 4.5 keV. As a diagnostic tool, we have taken the data in Fig. 5, and subtracted in quadrature the contribution to the width from electronic noise. These data have been fit to a power law as shown in Fig. 6.

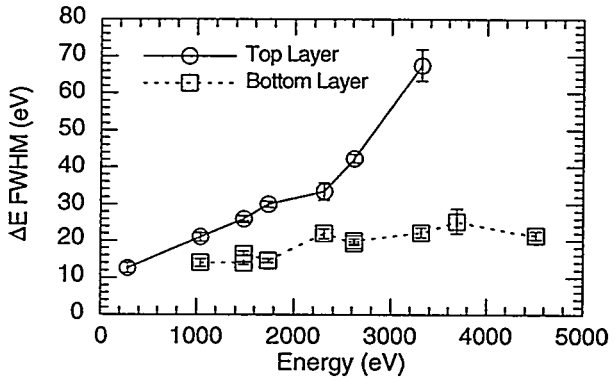

Fig. 5. The measured spectral resolution of the detector. The lines are drawn between the points for clarity.

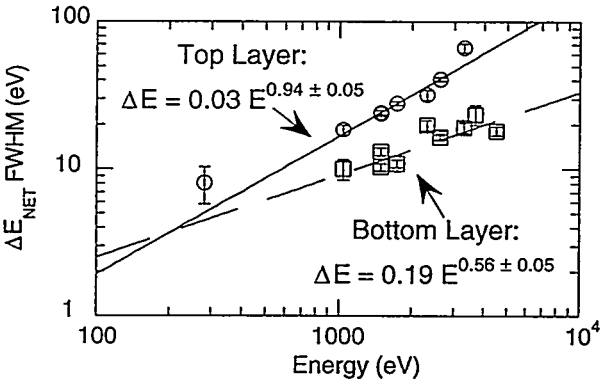

Fig. 6. The net resolution has been calculated by subtracting in quadrature the electronic noise from the measured resolution. A weighted power law fit is also shown.

V. Discussion

The overall linearity of the detector is rather good; the largest deviations from linearity are less than 3%. This is in contrast to the strong nonlinearity seen with a tin superconducting tunnel junction X-ray spectrometer that produced low energy escape peaks [12]. The nonlinearity that exists in our Nb/Al device is most significant at energies above 4 keV, particularly for the top layer. Note that the nonlinearity is in the form of an expansion, not compression of the observed spectra. At higher energies the pulses tend to be larger than predicted by a straight-line extrapolation of the pulse heights at lower energies. This would suggest that there is little self-recombination of the X-ray generated quasiparticles. On the other hand, we have observed that the higher-energy pulses tend to last longer than those produced by lower energy X rays. This effect is strongly dependent on the detector bias, temperature, and pulse integration time, and may be due to the effective increase in energy imparted to each quasiparticle when it tunnels across the barrier. Due to the electronic filtering, longer pulses will appear with slightly higher pulse heights.

The pulse heights and the resolution are also consistently higher for X-rays absorbed in the bottom layer. This suggests the bottom layer may be more uniform and contain less lattice defects and impurities. It is also possible that the top layer is more susceptible to trapping magnetic flux from unintentional transient current pulses through the junction and other sources.

The most dramatic evidence for a fundamentally different broadening mechanism in the two niobium layers is given by the power-law fits shown in Fig. 6. The resolution for X rays absorbed in the top layer is consistent with a linear dependence on energy. This linear dependence on energy is what we would expect if the dominant broadening mechanism is due to variations in pulse height with the position at which the X ray was absorbed.

On the other hand, the resolution for X rays absorbed in the bottom layer is consistent with a square root dependence on the energy. This is what we would expect if the resolution is limited by some statistical process such as variations in the number of quasiparticles produced, the number of times that each quasiparticle tunnels through the barrier during our measurement time, and the number of quasiparticles that are lost due to recombination or other mechanisms during our measurement time. The statistics of these processes have been discussed in [8] and [9].

Acknowledgment

We wish to thank R. C.. Dynes, John Rowell, John Clarke, Bernard Sadoulet and Sunil Golwala for valuable discussions.

References

[1] N. E. Booth, "Quasiparticle Trapping and the Quasiparticle Multiplier," *Appl. Phys. Lett.*, vol. 50, pp. 293-295, 1987.

2] H. Kraus, *et al.*, "Quasiparticle Trapping in a Superconductive Detector System Exhibiting High Energy and Position Resolution," *Phys. Rev. B*, vol. 231, pp. 195-202, 1989.

[3] A. T. Barfknecht, R. C. Ruby, and H. Ko, "A Simple and Robust Niobium Josephson Junction Integrated Circuit Process," *IEEE Trans. Mag.*, vol. MAG-27, pp. 970-973, 1991.

[4] S. E. Labov, *et al.*, "Superconducting Tunnel Junction Detectors Using Niobium X-ray Absorbers and Aluminum Quasiparticle Traps," *SPIE proc.*, vol. 1743, pp. 328-338, 1992.

[5] R. F. Broom, W. Kotyczka, and A. Moser, "Modeling of Characteristics for Josephson Junctions Having Nonuniform Width or Josephson Current Density," *IBM J. Res. Develop.*, vol. 24, pp. 178-187, 1980.

[6] E. P. Houwman, J. G. Gijsbertsen, J. Flokstra, and H. Rogalla, "On the suppression of the sidelobes of the supercurrent in small Josephson tunnel junctions," *Physica C*, vol. 183, pp. 339-344, 1991.

[7] C. A. Mears, S. E. Labov, and A. T. Barfknecht, "Energy-resolving superconducting X-ray detectors with charge amplification due to multiple quasiparticle tunneling," *Appl. Phys. Lett.*, vol. 63, pp. 2961-2963, 1993.

[8] C. A. Mears, S. E. Labov, and A. T. Barfknecht, "High-Resolution Superconducting X-Ray Detectors with Two Aluminum Traps," *J. Low Temp. Phys.*, vol. 93, pp. 561-566, 1993.

[9] D. J. Goldie, P. L. Brink, C. Patel, N. E. Booth, and G. L. Salmon, "The statistical noise due to tunneling in superconducting tunnel junction detectors," *Appl. Phys. Lett.*, vol. 64, pp. 3169-3171, 1994.

[10] L. J. Hiller, *et al.*, "Non-equilibrium dynamics in superconducting tunnel junction detectors," *SPIE proc.*, vol. 2280, pp. 382-392, 1994.

[11] C. A. Mears, *et al.*, "High-Resolution Superconducting X-Ray Spectrometers with Aluminum Trapping Layers of Different Thicknesses," *IEEE Trans. Appl. Supercon.*, vol. this volume, , 1994.

[12] A. Zehnder, C. W. Hagen, and W. Rothmund, "Superconducting Tunnel Junction Detectors," *SPIE proc.*, vol. 1344, pp. 286-294, 1990.